Three-dimensional scanning near field optical microscope (3D-SNOM) imaging of random arrays of copper nanoparticles: implications for plasmonic solar cell enhancement

Sabastine Ezugwu[1], Hanyang Ye[1], and Giovanni Fanchini[1,2]

[1]Dept. of Physics & Astronomy, Western University, London, ON N6A 3K7, Canada

[2]Dept. of Chemistry, Western University, London, ON N6A 5B7, Canada

1. Additional Experimental details

1.1. The deposition system

Copper nanoparticles (Cu-NPs) were grown by radio frequency (RF) magnetron sputtering of a copper target with argon ions in a vacuum chamber made of stainless steel cylinder equipped with facilities to control the deposition parameters. Figure S1 is a picture of the deposition system and the glove box (VAC, NEXUS, 100027 - 100062).

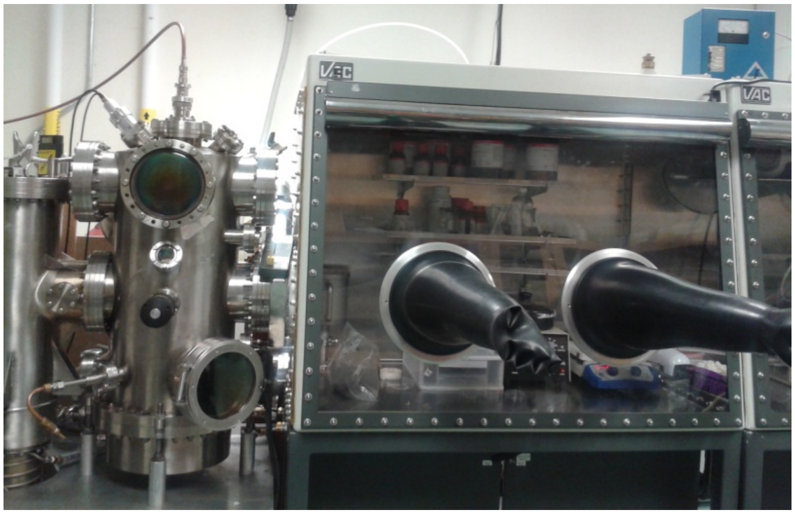

Figure S1 – Picture of the RF Sputtering system with glove box attached used for this work

The vacuum chamber has been coupled to the glove box, through a gate valve interconnect that allows for easy access to the chamber without necessarily exposing the system to the ambient conditions. The oxygen content in the glove box is monitored with an oxygen analyzer (DELTA corp. Trace Oxygen Analyzer, FA3555OSA). The substrates are mounted on a 3½ inch square substrate holder, made of stainless steel base and brass cover. The sample stage is 6 inches from the sputtering cathode and the samples can be shaded during the transitory corresponding to the start up of the discharge with the aid of a rotary manipulator, as shown schematically in Figure S2.

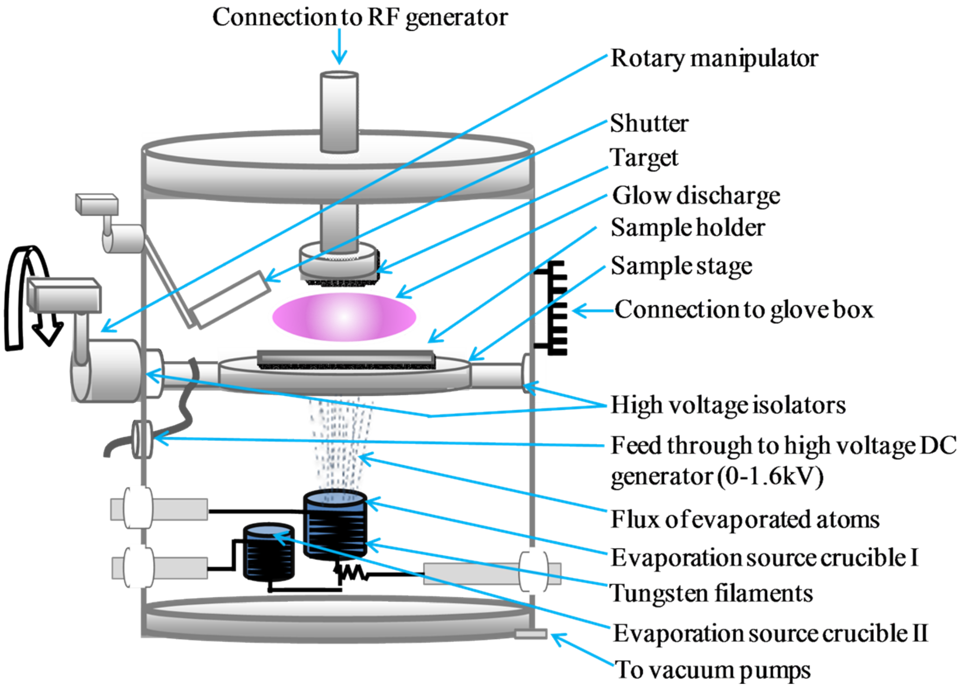

Figure S2 – Schematics of the deposition chamber showing the RF sputtering system for NPs deposition and thermal evaporation unit used to deposit metallic cathode on solar cells. The orientation of the sample relative to the source is controlled with the rotary manipulator.

The attachment to the rotary manipulator as well as the chamber is designed to ensure that the sample stage is electrically floating in the absence of additional electrical connections that are placed only when the substrate is DC – biased. A dc power supply (CANBERRA 3010, rated for 1600 V and 5 mA max) has been used to apply DC biasing voltage to the substrate. The sputtering cathode serves as the holder for the sputtering target and couples the radio frequency power to chamber.

The thermal evaporation system is installed at the lower part of the chamber and used for evaporation of solar cells metallic cathode. The unit is powered by HP 6466C DC power supply with output of 0 – 16V and 0 – 600A. With two installed evaporation source crucibles, the time required to re-load sources and subsequent pumping down of the chamber are eliminated, especially in the case of interdigited bilayer metallic contacts discussed in section 2.3.

1.2 Copper nanoparticle deposition

The deposition was carried out on microscope glass and Si substrates. With the aid of a diamond cutter, the substrates are cut into ½ x ½ inch square that fit into the substrate holder. This is followed by ultrasonic cleaning of all of the substrate in water with detergent, acetone and methanol for 15 minutes each. The substrates are then exposed to UV/ozone radiation (UV3 Novascan) for 20 minutes to get rid of any oxide residues. UV/ozone treated substrates are immediately introduced into the glove box. From the glove box, the substrates are placed on the deposition substrate holder and covered with a shadow mask which ensures that they remain in position even when turned upside down inside the chamber.

1.3 Variation of process parameters and deposition conditions of copper nanoparticles

All the sputtering operation was carried out at a base vacuum better than $5x10^{-7}$ torr. Sufficiently low vacuum is required in the deposition chamber prior to sputtering to reduce the effect of contamination and oxidation, especially for the case of Cu-NP. Low pressure is also desirable during the actual sputtering operation in order to raise the mean free path of the sputtered species and increase the sputtering rate. Sputtering is initiated by allowing a flow of argon gas into the deposition chamber, at a flow rate determined by the mass flow controller (OMEGA, FMA5508, range: 0 – 100mL/min). The substrate can float, biased or connected to ground as may be desired. As shown in Table S1, the sample used for our 3D-SNOM study was deposited at increasing argon flow rate. By varying argon flow rate, the change in gas flow also varied the gas pressure in the deposition chamber as shown in Figure S3.

Table S1 – Sputtering parameters for deposition of Cu-NPs at different argon flow rates

Ar flow rate (SCCM)	RF power (W)	Sputtering Time (min)	Substrate bias voltage (V)
6	75	3	- 400
9	75	3	- 400
15	75	3	- 400
18	75	3	- 400
20	75	3	- 400

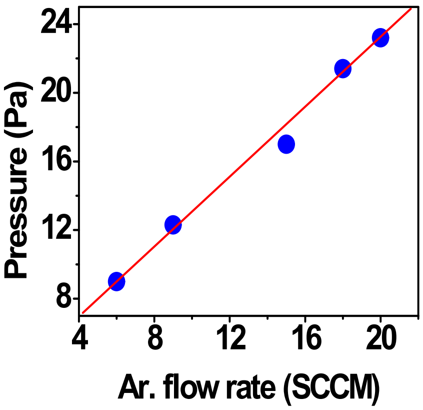

Figure S3 – Relationship between Ar flow rate and chamber pressure in our growth chamber

1.4 RF Magnetron Sputtering Deposition of the SiO_2 spacer

Our RF magnetron sputtering system was also utilized for sputtering SiO_2 thin films used as a spacer atop of the Cu-NPs as discussed in sections 2.2 and 2.3. This was accomplished by attaching a 2-inch diameter silicon oxide target to our cathode electrode in place of the copper target. Depositions of SiO_2 were carried out at 90W RF power and 8 Pa Ar pressure. We determined the deposition rate in these conditions by partially masking the substrate with Kapton Tape in a set of films sputtered for different times from 30 mins to 600 mins. The height of the films relative to the masked portion of the substrate was then measured using contact-mode 10 × 10 μm AFM scans. A deposition rate of 5.4 nm/min was determined in this way. Figure S4 shows a plot of the thickness of SiO_2 against the sputtering time. These samples were used for the fabrication of our thin film plasmonic solar cells.

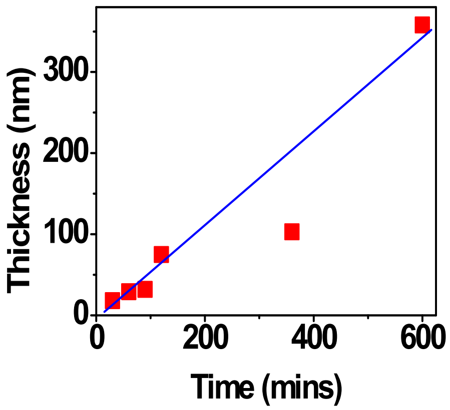

Figure S4 – Deposition rate of RF-sputtered SiO_2 in the conditions used to prepare the spacer

2. Additional Results

2.1 Nucleation of copper nanoparticles

We obtain high quality copper island in-situ, during the sputtering operation, by controlling the deposition rate via negative dc-bias voltage applied to the substrate and ex-situ, through thermal treatment of interconnected copper particles. To demonstrate this, we show in Figure S5 the scanning electron microscopy (SEM) images of copper nanoparticles deposited for 3 minutes at 75W RF power and 12 Pascal sputtering chamber pressure. Panel (a) of Figure S5 is the SEM image of in-situ fabricated Cu islands obtained through reduced sputtering rate achieved through a dc-bias voltage of – 400V applied to the substrate. In this case, the deposition of Cu-NPs begins with the nucleation of copper nuclei on the substrate (heterogeneous nucleation). With the substrate exposed to the flux of neutral Cu atoms during the sputtering operation, the atoms stick on the substrate by nucleation. In this early stage, the prior nuclei incorporate impinging atoms and grow in size. As shown in panel a, the morphological evolution is characterized by a transition from high density but uniformly distributed species to isolated but relatively large sized Cu particles. Panel d of Figure S5 shows that the distribution of Cu particles in this sample is skewed towards smaller particles diameter.

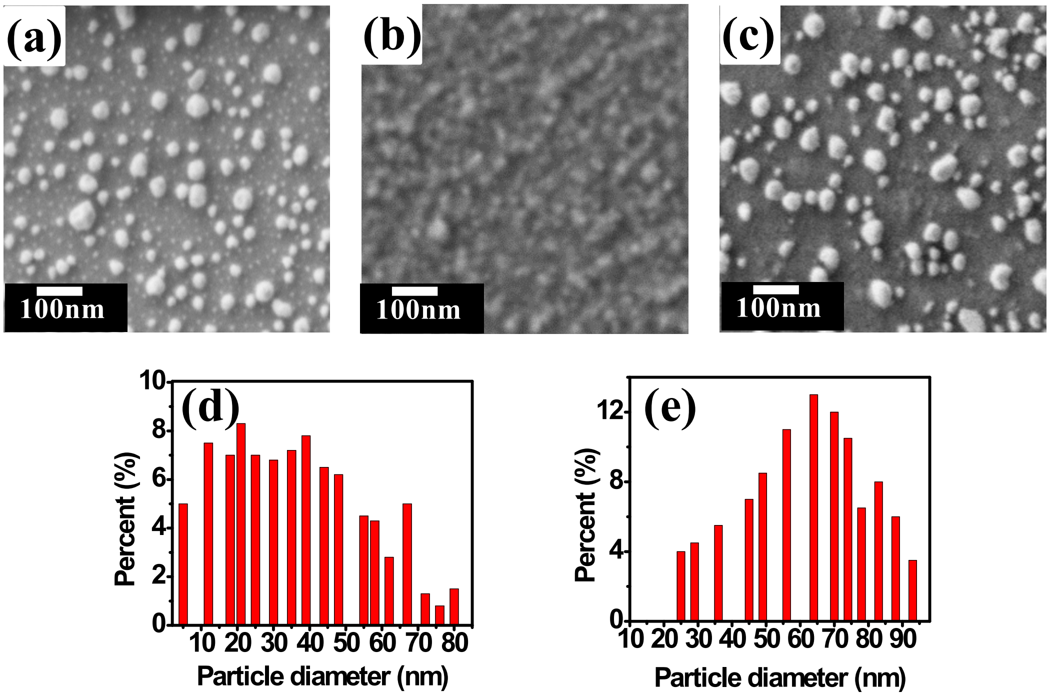

Figure S5 – SEM images of Cu-NPs nucleated on glass substrate (a) in-situ via substrate DC bias voltage of - 400V, (b) as inter-connected particles in the absence of bias voltage and (c) ex-situ by thermal treatment in the glove box at 300^{o}C for 2 hours. (d) and (e) are the respective size distributions of Cu-NPs shown in Panel (a) and (c).

In the absence of any substrate bias voltage, the flux of copper atoms impinging on the substrate grow in both in- and out-of-plane direction with further deposition time. As such, coalescence phenomenon favors the formation of planar or continuous film as can be observed in the SEM image of Figure S5 (b). Consequently, thermal treatment of as-grown interconnected Cu-NPs is required to initiate further nucleation sufficient for island formation. Panel c of Figure

S5 gives the SEM image of the same sample shown in panel b after thermal annealing was carried out in the glove box at 300^{o}C for two hours. It is evident that the aggregates and semi-connected network of Cu-NPs observed in panel b completely coalesce during thermal treatment in inert condition. Ex-situ particle coalescence has been thermally activated by annealing in oxygen free environment. Figure S5 (e) shows the dispersion of Cu-NPs obtained from the sample shown in panel c. The figure shows that the particle dispersion follows a Gaussian distribution.

2.2 3D-SNOM results and mean particle size and dispersion of Cu-NPs

In this section, we present the results of our 3D-SNOM measurement on the set of samples deposited at different chamber pressures as in Table S1. Image J, a free program package for image processing and manipulation [S1] was used to process the particle morphology acquired simultaneously from the (x-y) SNOM scans to obtain the size dispersion of the particles. Prior to particles size determination, the image is first calibrated in order to replicate the magnification of the source in the analyzed image. Although it is difficult to determine the sizes of all the particles very accurately especially in the case of connected Cu-NPs of small size, careful adjustment of the particles size threshold allows for better identification and counting of all the particles being analyzed. From the average size *S*, the average diameter *d*, is calculated for isolated Cu-NPs:

$$d = 2 \cdot \sqrt{S/\pi} \qquad \text{(S1)}$$

The complete set of our 3D-SNOM measurements, including the morphology, optical image, 3D intensity map and the profiles are presented in Figures S6 to S9, for the samples deposited under different chamber pressure shown in Table 1. These results were discussed in sections 2.2.

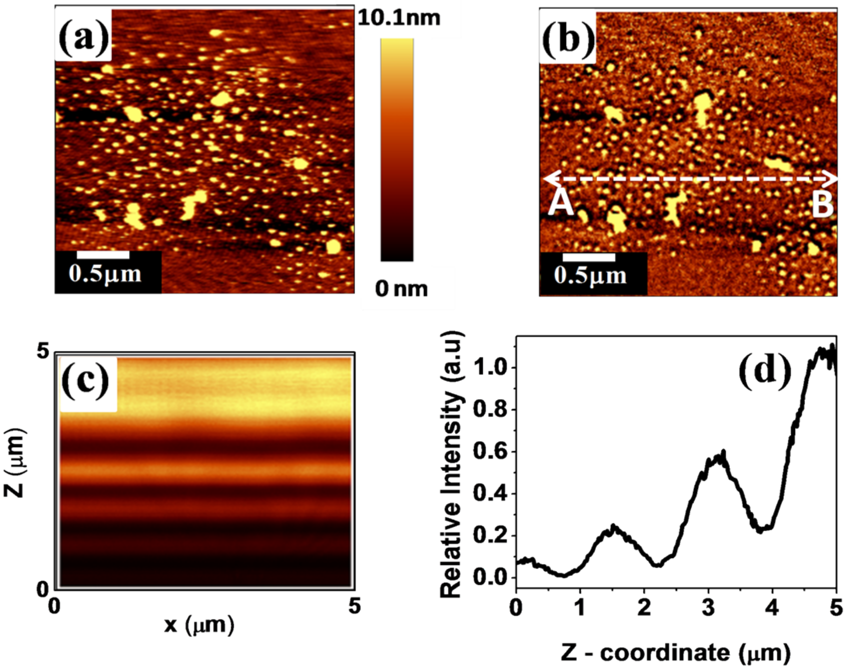

Figure S6 – (a) Topographic and (b) optical images obtained simultaneously from SNOM measurement on Cu-NPs sputtered at 9 Pa chamber pressure. (c) 3D-SNOM intensity mapping performed along the A – B cross section shown in panel (b). (d) Intensity profile showing the positions of constructive (maxima) and destructive (minima) interference of light scattered from Cu-NPs.

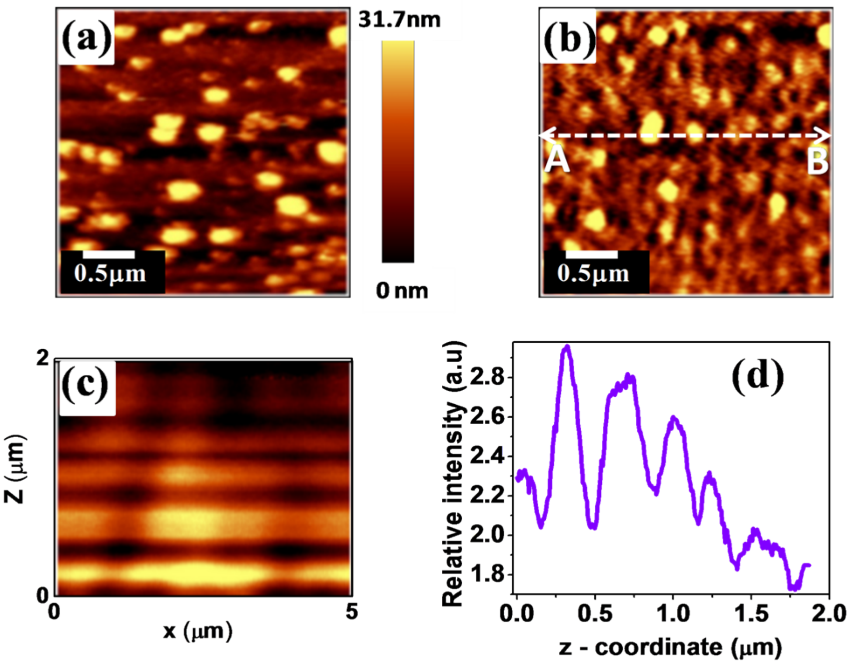

Figure S7 – (a) Topographic and (b) optical images obtained simultaneously from SNOM measurement on Cu-NPs sputtered at 17 Pa chamber pressure. (c) 3D-SNOM intensity mapping performed along the A – B cross section shown in panel (b). (d) Intensity profile showing the positions of constructive (maxima) and destructive (minima) interference of light scattered from Cu-NPs.

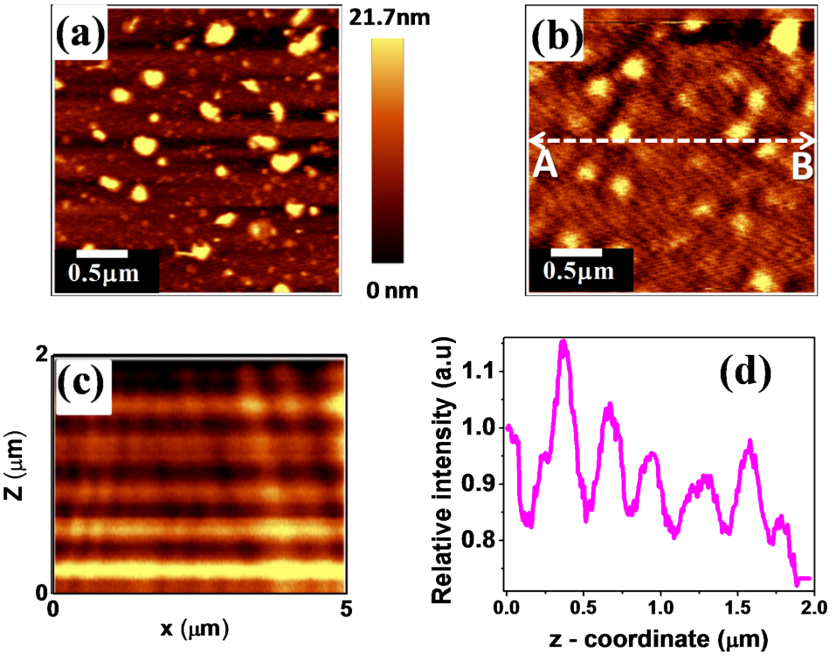

Figure S8 – (a) Topographic and (b) optical images obtained simultaneously from SNOM measurement on Cu-NPs sputtered at 21 Pa chamber pressure. (c) 3D-SNOM intensity mapping performed along the A – B cross section shown in panel (b). (d) Intensity profile showing the positions of constructive (maxima) and destructive (minima) interference of light scattered from Cu-NPs.

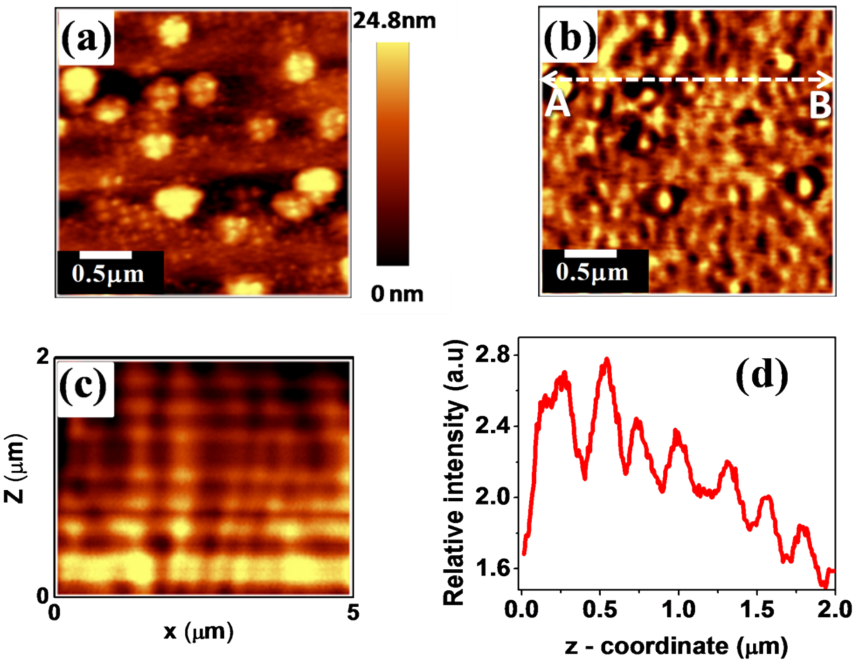

Figure S9 – (a) Topographic and (b) optical images obtained simultaneously from SNOM measurement on Cu-NPs sputtered at 23 Pa chamber pressure. (c) 3D-SNOM intensity mapping performed along the A – B cross section shown in panel (b). (d) Intensity profile showing the positions of constructive (maxima) and destructive (minima) interference of light scattered from Cu-NPs.

The variation in the chamber pressure also affects the size and degree of dispersion of Cu-NPs as demonstrated in Figure S10. Particles grown at higher pressures have larger particle diameter and are less densely populated compared to Cu-NPs deposited at lower pressures. The increase in the particles size can be attributed to increased nucleation time from low deposition rate, resulting from the change in mean free path l, of the gaseous Cu atoms in the plasma with chamber pressure P, i.e. l (cm) $\propto 1/P$ (Pa) [S2]. From this relation, it is seen that higher pressures, obtained at higher argon flow rates, result in smaller mean free path of the gaseous Cu atoms. Consequently, the sputtered copper atoms are prone to a large number of collisions and have a higher probability of agglomeration before impinging the substrate. Besides, the mean free path of the gaseous species in the chamber influences the rate at which Cu target is sputtered. Argon ions lose energy by collisions when they are accelerated close to the target [S3]. Therefore the lower the pressure, the more particles involved in the coalescence phenomena that are taking place in the proximity of the substrate surface. This explains the high density of particles deposited at lower pressures.

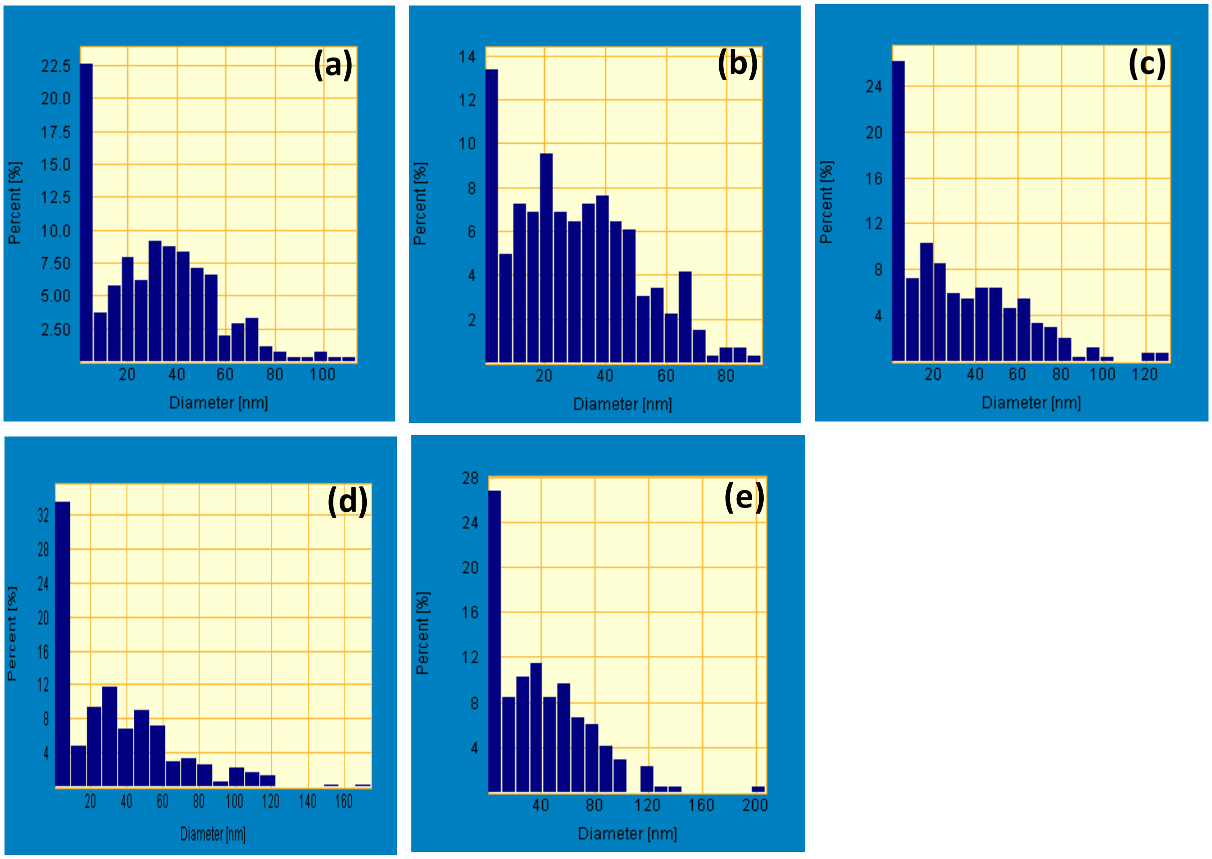

Figure S10 – Size dispersion of Cu-NPs deposited in constant RF power at different chamber pressures of (a) 9, (b) 12, (c) 17, (d) 21 and (e) 23 Pa

In view of the above analysis, one can say that the size distribution of Cu-NPs, shown in Figure S10, results from different mean free path. The mean diameter of the particles is presented in Figure S11 as a function of pressure. Coalescence and increase in size is clearly favored at higher sputtering pressure.

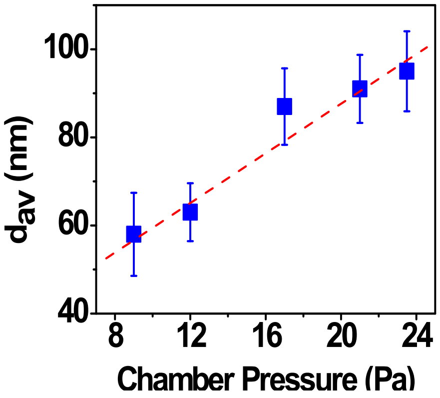

Figure S11 – Average diameter of Cu-NPs versus sputtering chamber pressures

2.3 Optical transmittance of Cu-NPs

Optical transmittance is another important property that can determine the performance of our nanoparticles as a plasmonic enhancement layer. Below, we compare the optical property of these Cu-NPs, deposited at different chamber pressures. Figure S12 shows that the transmittance increases with increasing chamber pressures and at higher pressures, the NPs produce increased transmittance enhancement peaks that can be attributed to the metallic behavior in these samples – the morphology of the Cu-NPs shows that the nanoparticles are inter-connected. In Figure S13, we show that the position of the transmittance peak (obtained from Figure S12) decreases to 548 nm at 17 Pa and then increases. However, the intensity of the peaks monotonically increases as the sputtering chamber pressure increases, which led to samples with lower density of particles.

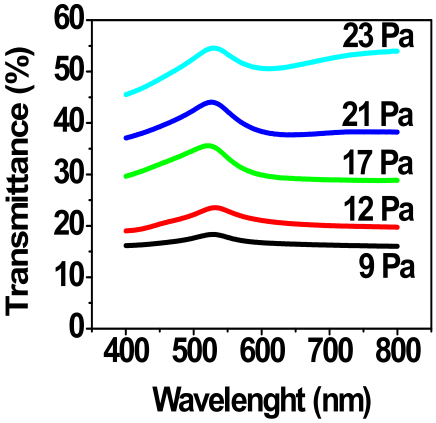

Figure S12 – Transmittance vs. wavelength for Cu-NPs deposited by RF magnetron sputtering at different chamber pressures

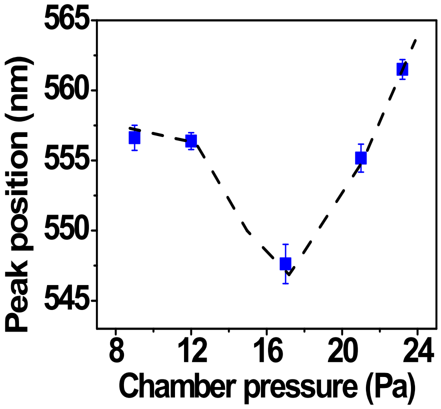

Figure S13 – Transmittance spectra peak positions, T_{max} obtained from Figure S11, for Cu-NPs deposited by RF magnetron sputtering at different chamber pressures.

References

[S1] http://rsb.info.nih.gov/ij/

[S2] V. Chawla, R. Jayaganthan, R. Chandra, *J. Mater. Sci. Technol*. **2010**, 26(8), 673

[S3] T. Ghodselahi, M. A. Vesaghi, A. Shafiekhani, A. Baradaran, A. Karimi, Z. Mobini, *Surf. & Coatings Tech.* **2008**, 20, 2731